

# Magnetization reduction by non-linear effects

V. V. Naletov, G. de Loubens, and O. Klein

*Service de Physique de l'État Condensé,*

*CEA Orme des Merisiers, F-91191 Gif-Sur-Yvette*

(Dated: May 23, 2019)

## Abstract

In current-driven magnetization dynamics, the excitation of spatially inhomogeneous spin-waves, which are degenerate with the uniform motion, should arise from the neglected non-linear coupling in the microscopic spin torque model. This effect is illustrated by new measurements of  $M_z$ , the time averaged magnetization, at the saturation of the main resonance in ferromagnetics. It is shown that  $M_z$  drops brutally when saturation effects set in. It results from a rapid growth of the degenerate magnons and the effect is explained in terms of a vanishing decay rate of the spin-waves created by the non-linear coupling.

Recent experiments about the anomalous switching behavior [1, 2, 3] of spin-valve structures pumped by large dc-current under applied field have cast some doubts [3] on the validity of the spin-torque (ST) model [4, 5]. The latter model has been proposed to describe current-driven spin-waves excitation in magnetic multilayers. It has received much experimental [6] and theoretical [7] attention owing to the potential application in spin electronic devices. The ST model relies on the transfer of spin from a polarized electron current to a magnetic layer of magnetization  $M$ . Spin-waves instabilities occur when the deposited torque compensates the viscous component  $G\dot{M}$  in the Landau-Lifshitz equation ( $G$  is the Gilbert damping coefficient). The ST is based on a microscopic description of the dynamics valid only at a scale smaller than the exchange length (the scale of the macrospin approximation). Important physical aspects are thus left out by neglecting spatially inhomogeneous spin-waves and their coupling to the uniform precession through the depolarization field [8]. It will be shown below that the increase of magnons' occupation numbers, observed recently in the telegraphic noise [1, 2], is likely an increase of degenerate magnons (*i.e.* oscillating at the uniform mode frequency but with a larger wavevector) arising from the neglected non-linear coupling in the ST model rather than an increase of thermal magnons occupation.

By analogy with the case of spin injection at the switching threshold, we use high levels of microwave excitation to drive the magnetization dynamics at large precession angles where saturation effects set in. Here second order effects in the demagnetizing energy become important and they destroy the independence of the degenerate spin-waves modes. We will present our results obtained at room temperature on an yttrium iron garnet (YIG) sample, shaped into a disk of diameter  $D = 160\mu\text{m}$  and thickness  $S = 4.75\mu\text{m}$  and perpendicularly magnetized in a static field of  $H_{\text{ext}} = 5.3\text{ kG}$ , *i.e.* well above the YIG saturation field. The relaxation mechanisms in the limit of infinitesimal excitations have been completely characterized in a previous paper [9]. This letter reports the measurement of both the longitudinal and transverse components of the magnetization at the saturation of the main resonance. It is found that  $M_z$  drops brutally when saturation effects set in. It results from a rapid growth of the non-equilibrium degenerate magnons. The experimental data are in qualitative agreement with the Suhl's model describing the saturation of the main resonance in the presence of two-magnon scattering [10]. The inclusion of these non-linear effects inside the microscopic ST model provides an additional mechanism to reverse the magnetization through a reduction of the time averaged magnetization  $\langle M \rangle_t = M_z$  for the configuration

anti-parallel to the deposited spin.

In ferromagnetic resonance, the uniform rf field generated by the synthesizer preferentially couples to the longest wavelength modes available, i.e. the magnetostatic modes. At  $\omega_0/2\pi = 10.47\text{GHz}$ , it excites the main resonance of our disk, which has a transverse wavevector  $k_0 \approx \pi/D$  and is referred hereof as the uniform precession because its phase is coherent throughout the sample. The power reflected from the sample at resonance is detected by a microwave diode whose signal is proportional to the imaginary part of the transverse susceptibility  $\chi''$  (the latter quantity is spatially averaged over the sample volume). The number of uniform magnons is  $n_u = \frac{1}{2}|u_0|^2$ , with  $u_0 = \chi''h/M_s$ ,  $h$  being the circularly polarized amplitude of the rf field and  $M_s$  the saturation magnetization at thermal equilibrium. The energy relaxation rate of the uniform precession will be written  $\eta_0$  (our definition is twice as large as the amplitude relaxation rate used in Suhl's paper [8, 10]). But the uniform precession is also degenerate with other spin-waves motions as shown in Fig.1a. This is true for any samples of finite aspect ratio [11]. Inhomogeneities, impurities or crystal defects, lead to a linear coupling between the degenerate modes. In the canonical formalism, this coupling is described by a scattering matrix whose most important components are those that couple the uniform precession to spin-waves of the form  $u_k e^{-i\omega_k t}$  of identical energies ( $\omega_k = \omega_0$ ) but different wavevectors  $k \gg k_0$ , propagating at an angle  $\theta_k$  from the normal of the disk,  $\overline{\eta}_k$  being their average decay rate to the thermodynamic equilibrium. Fig.2 shows the energy flow diagram between the modes with  $\eta_{sp}$  the decay constant of the uniform precession due to inhomogeneity scattering.

In addition to this linear coupling, there is also a non-linear coupling inside the degenerate band. The leading term is the coupling between uniform and degenerate pairs. We will call this the first order approximation. As shown by Suhl, degenerate modes of equal and opposite wave vectors  $(+k, -k)$  are coupled by matrix elements proportional to  $\xi_k n_u$  in the dipolar Hamiltonian. For perpendicularly magnetized films, the maximum amplitude of the non-linear coupling coefficient is  $\xi_{k_{\max}} = 2\pi M_s \approx 900\text{G}$ , a result that is derived from the Holstein-Primakoff diagonalization and is explained in reference [8]. The first pairs that grow unstable (Fig.1b) propagate at  $\theta_k = 0$  (along the  $z$  direction) with a wavevector  $k_{\max} \approx 6.3 \times 10^4 \text{cm}^{-1}$  derived from the equality  $\omega_k = \omega_0$  (Fig.1a). The important consequence of that non-linear coupling is the saturation of the uniform mode that may be described as a reduction of the loss parameter  $\eta_z$  of spin-waves propagating along the normal of the

disk. The apparent decay rate  $\tilde{\eta}_z = \eta_z/f(n_u)$  of these pairs decreases with power and  $f(n_u) = 1/\sqrt{1 - n_u^2/n_c^2}$  is the non-linear correction derived by Suhl [8]. The critical number of uniform magnons  $n_c = \frac{1}{2}\chi_0''^2 h_c^2/M_s^2$  depends on  $\chi_0'' = 2\gamma M_s/(\eta_0 + \eta_{sp})$ , the low power susceptibility, and  $h_c^2 = \frac{(\eta_0/2 + \eta_{sp}/2)^2}{\gamma^2} \frac{\eta_z}{2\xi_k}$  the saturation power. In the following, we propose to measure the occupation numbers of these unstable spin-waves pairs arising from the non-linear interactions.

Complementary informations are obtained by measuring  $\Delta M_z = M_s - M_z$ , the change of longitudinal component. It is proportional to  $n_t = \frac{1}{2} \sum |u_k|^2$ , the total number of magnons excited by the rf power. The thermal magnons' occupation numbers are accounted for in  $M_s$ . In all our discussion the number of thermal magnons will remain constant and fixed by the lattice temperature. In this paper we propose to use the sensitivity of Magnetic Resonance Force Microscopy to follow  $M_z$  up to nanoWatt excitations (Fig.1c). A small permanent magnet is affixed at the end of a flexible cantilever and placed above the sample. Changes of  $M_z$  at resonance produce a modification of the force applied to the tip.

We plot in Fig.3 the rf field dependence of both  $\chi''$  and  $\Delta M_z/h^2$  evaluated at resonance. We observe that the microwave susceptibility data exhibits the well known premature saturation behavior at  $h_c = 5\text{mG}$ . In the presence of two-magnons scattering, it was shown that the susceptibility obeys the implicit equation [10]

$$\chi'' = \frac{2\gamma M_s}{\eta_0 + \eta_{sp} f(\frac{1}{2}\chi''^2 h^2/M_s^2)}. \quad (1)$$

In Suhl's original paper, the expression is derived from a first order approximation. Since non-linear effects only modify the coupling between degenerate modes, Eq.1 can be valid at all higher order, provided that the corrections are introduced in  $f$  [12]. Below we try to compare quantitatively our data to the profile predicted by Eq.1. We start from our measurements of the relaxation in the linear regime [9], which gives the values of  $\eta_0/\gamma = 1.07\text{G}$ ,  $\eta_{sp}/\gamma = 0.2\text{G}$  and  $\overline{\eta}_k/\gamma = 0.65\text{G}$  assuming that the magnons can be arranged within the schematic distribution of Fig.2. The value of  $\overline{\eta}_k$  is slightly larger than the damping coefficient of  $k_0$  magnons ( $0.45\text{G}$  [9]), a result consistent with the parallel pumping experiments [13]. Assuming, as in Suhl's paper [10], that  $\eta_k$  is independent of  $k$  (in particular  $\eta_z = \overline{\eta}_k$ ), one calculates a value for  $h_c$  that is much higher than the one observed experimentally. This suggests that the decay rate of the degenerate magnons must get smaller as  $\theta_k$  approaches the normal direction of the disk [14]. So we have fitted the value of  $\eta_z$  to the measured

value of  $h_c$  and the best agreement is obtained for  $\eta_z/\gamma = 0.15G$ . Such a discrepancy has already been observed [14] and the effect might be enhanced by our thin film geometry, where  $z$ -directed magnons are reflected back on the substrate. We have displayed in Fig.3 the power dependence of  $\chi''$  predicted by Eq.1 using the first order expression for  $f$ , with no additional fitting parameter. The model predicts properly the shape and in particular the smearing out of the singularity at  $h_c$  (cf. Fig.3).

In contrast with the monotonic decrease of  $\chi''$ , the power dependence of  $\Delta M_z/h^2$  exhibits a peak. This result seems at odds with the decreasing absorbed power observed in the transverse pumping experiment. Furthermore, a dependence of the form  $\Delta M_z \propto h^n$  with  $n > 2$  has never been established experimentally before.

Direct calculation of  $\Delta M_z/M_s = \frac{1}{2} \sum_{\{k\}} |u_k|^2$ , where the sum runs over all possible  $k$  values, is difficult [8]. A clever way to circumvent this difficulty, is to look at the energy balance under stationary conditions [12]. The absorbed power  $P_{\text{abs}} = 2\omega M_s u_0 h$  per unit volume must match the dissipated power in the sample  $P_{\text{diss}} = M_s \frac{\omega_0}{\gamma} \sum_{\{k\}} \eta_k |u_k|^2$  [12, 14]. The schematic shown in Fig.2 splits up the sum in three categories. There are the uniform  $\eta_0 |u_0|^2$ , the inhomogeneities  $\overline{\eta}_k \sum_{\{k \neq 0\}} |u_k|^2 = \eta_{sp} |u_0|^2$  [12] and the non-linear  $\eta_z \sum_{\{k_{\text{max}}\}} |u_k|^2$  contributions. For the schematic in Fig.2, the energy balance,  $P_{\text{abs}} = P_{\text{diss}}$  (valid at any order) then becomes:

$$\frac{\Delta M_z}{\Delta M_{z0}} = \frac{\eta_0 + \eta_{sp}}{\overline{\eta}_k + \eta_{sp}} \frac{\overline{\eta}_k}{\eta_z} \left\{ \left( \frac{\chi''}{\chi_0''} \right) - \left( \frac{\chi''}{\chi_0''} \right)^2 \right\} + \left( \frac{\chi''}{\chi_0''} \right)^2, \quad (2)$$

with  $\Delta M_{z0} = \left(1 + \frac{\eta_{sp}}{\overline{\eta}_k}\right) \frac{2\gamma^2 M_s}{(\eta_0 + \eta_{sp})^2} h^2$  the variation of the longitudinal component in the linear regime. The solid line in Fig.3 is the peak predicted by Eq.2. Experimentally we find that the enhancement of  $\Delta M_z/h^2$  begins at much lower power than  $h_c$ . We have omitted so far the spatial non-uniformity of the main resonance in order to keep the discussion simple. For small size samples, the angle of precession is larger at the center of the disk than at the boundary [15]. Changes in the profile are expected when different locations of the sample hit the saturation threshold. The rise of  $\Delta M_z/h^2$  coincides with the saturation of the central part of the disk while the spatially averaged transverse susceptibility  $\chi''$  drops at higher power, approximately when the peripheral zone saturates. The dashed line in Fig.3 is the predicted behavior when Eq.2 is weighted by the spatial profile of  $\Delta M_z$ . The good agreement with the data suggests that the enhancement of  $\Delta M_z/h^2$  below  $h_c$  is a finite size effect.

Further insight can be obtained by combining Eq. 2 with the expression of  $\chi''$  (Eq.1). We then obtain the relation  $n_u/n_t$  is proportional to  $\tilde{\eta}_z/\overline{\eta}_k$ . So the number of excited spin-waves can grow indefinitely without energy cost when  $\tilde{\eta}_z \rightarrow 0$ . The peak observed in  $\Delta M_z/h^2$  is thus just a signature of the decreasing decay rate of the pairs excited by non-linear effects. To illustrate the power dependence of  $\tilde{\eta}_z$  with our data, we have plotted in Fig.4 the ratio of  $\chi''^2 h^2$  over  $\Delta M_z$ . The experimental data in Fig.4 are thus compared with the first order approximation of  $f$ . As predicted by the model, we see that  $\tilde{\eta}_z$  starts to decrease below  $h_c$ , in agreement with recent BLS measurements [16]. It is also interesting to notice that the decrease is monotonic and there is no singularity at  $h_c$ . It extends to the  $h > h_c$  region and the lifetime instability is approached asymptotically when  $\eta_{sp} \neq 0$ . At large power  $h^2 \gg h_c^2$ , the Eq.2 reduces to  $\Delta M_z \propto \chi'' h^2$  as first found by Suhl (see appendix of ref[8]). This means that  $\Delta M_z/h^2$  follows the decrease of  $\chi''$  when all degenerate modes are saturated too.

We now turn our attention to the interpretation of the spin-current data. The recent observation of telegraphic noise [1, 2, 3] when the non-equilibrium spin transfer is compensated by an applied field has led to the emergence of new models based on an effective spin-temperature in analogy with the Néel-Brown model. The effective temperature describes the increase of incoherent magnons when large precession are induced. We first review the coupling mechanism between current and spin-wave excitations [17]. Spin deposition into a ferromagnetic layer can only occur through stimulated emission. At microwave frequencies, the probability for spontaneous emission ( $\propto \omega^3$ ) is too small to be significant compared to the probability for stimulated emission ( $\propto 1/\omega$ ). This means that a spin flip process must involve the low-lying magnons excitation that are degenerate with the normal modes of the system, i.e. the uniform precession [18] (low-energy thermal magnons are also more numerous at  $\omega_0$  [19]). Translated into the language of our diagram of Fig.2, it means that the external pumping (the current) is not only coupled to the uniform precession but also to the modes that are degenerate with  $\omega_0$  [17]. We argue here that, although the ST model describes the microscopic mechanism for spin-waves excitation, an additional process is the surge of non-equilibrium magnons at the switching threshold, which occurs inside the degenerate magnons manifold (as oppose to thermal magnons occupation) through the neglected non-linear coupling. The probability that the injected spins scatter inside the ferromagnetic layer follows  $n_t$ , the total number of degenerate magnons at  $\omega_0$ . It increases dramatically as soon as one degenerate mode saturates because it forces the infinite growth

of  $z$ -directed magnons through a vanishing decay rate ( $\tilde{\eta}_z \rightarrow 0$ ). The consequence is a reduction of the time averaged magnetization  $\langle M \rangle_t = M_z$  for the configuration anti-parallel to the deposited spin. This provides an additional mechanism to reverse the magnetization. Final assistance might come from thermally activated switching [1] or chaotic dynamics [20] but in any case the thermal energy available is the *lattice* temperature. We insist about the importance of the distinction between degenerate ( $\mu\text{eV}$  excitation) and thermal (meV excitation) magnons. The coupling between the magnons and the lattice is excellent for conducting samples and it should not be modified by the current. In the non-linear model, the growth of the non-equilibrium magnons population is not due to a change of the relaxation mechanism to the lattice but to a change of the coupling between modes of identical frequency (Fig.2). The redistribution takes place inside the degenerate magnons manifold, which means that the total energy is conserved.

We are greatly indebted to J. Ben Youssef, V. Charbois, C. Fermon and O. Acher for their help and support. This research was partially supported by the E.U. project M<sup>2</sup>EMS (IST-2001-34594) and the Action Concertée Nanoscience NN085..

- 
- [1] E. B. Myers, F. J. Albert, J. C. Sankey, E. Bonet, R. A. Buhrman, and D. C. Ralph, Phys. Rev. Lett. **89**, 196801 (2002).
  - [2] S. Urazhdin, N. O. Birge, W. P. Pratt, Jr., and J. Bass, Phys. Rev. Lett. **91**, 146803 (2003).
  - [3] J.-E. Wegrowe, Phys. Rev. B **68**, 214414 (2003).
  - [4] J. C. Slonczewski, J. Magn. Magn. Mater. **159**, 1 (1996).
  - [5] L. Berger, Phys. Rev. B **54**, 9353 (1996).
  - [6] E. B. Myers, D. C. Ralph, J. A. Katine, R. N. Louie, and R. A. Buhrman, Science **285**, 867 (1999).
  - [7] X. Waintal, E. B. Myers, P. W. Brouwer, and D. C. Ralph, Phys. Rev. B **62**, 12317 (2000).
  - [8] H. Suhl, J. Phys. Chem. Solids **1**, 209 (1957).
  - [9] O. Klein, V. Charbois, V. V. Naletov, and C. Fermon, Phys. Rev. B (Rapid Comm.) **67**, 220407 (2003).
  - [10] H. Suhl, J. Appl. Phys. **30**, 1961 (1959).
  - [11] M. J. Hurben and C. E. Patton, J. Appl. Phys. **83**, 4344 (1998).

- [12] E. Schlömann, Phys. Rev. **116**, 828 (1959).
- [13] R. C. LeCraw and E. G. Spencer, J. Phys. Soc. Japan, Suppl. (B1) **17**, 401 (1962).
- [14] R. C. Fletcher, R. C. LeCraw, and E. G. Spencer, Phys. Rev. **117**, 955 (1960).
- [15] V. V. Naletov, V. Charbois, O. Klein, and C. Fermon, Appl. Phys. Lett. **83**, 3132 (2003).
- [16] H. Y. Zhang, P. Kabos, H. Xia, P. A. Kolodin, and C. E. Patton, Phys. Rev. B **61** (2000).
- [17] S. Urazhdin, Phys. Rev. B **69**, 134430 (2004).
- [18] S. I. Kiselev, J. C. Sankey, I. N. Krivorotov, N. C. Emley, R. J. Schoelkopf, R. A. Buhrman, and D. C. Ralph, Nature **425**, 380 (2003).
- [19] N. Stutzke, S. L. Burkett, and S. E. Russek, Appl. Phys. Lett. **82**, 91 (2003).
- [20] M. Ye, D. E. Jones, and P. E. Wigen, J. Appl. Phys. **73**, 6822 (1993).

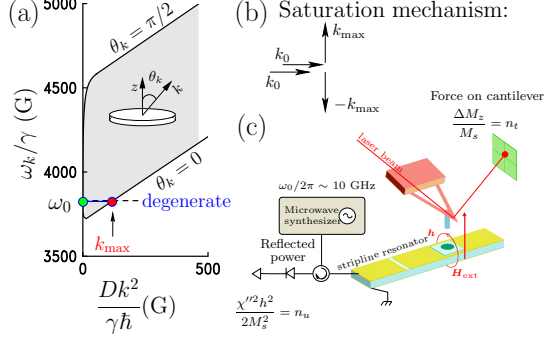


FIG. 1: (a) Spin-waves dispersion: the shaded area is the magnon manifold ( $D$  is the exchange constant). (b) At  $h_c$ , two quanta of the uniform precession break down into a degenerate spin-waves pair  $(+k_{\max}, -k_{\max})$  propagating at  $\theta_k = 0$ . (c) Block diagram of the experimental apparatus. A Magnetic Force Resonance Microscope, placed  $\ell = 100\mu\text{m}$  above the sample, is used to measure  $n_t$  while a standard microwave setup measures simultaneously  $n_u$ .

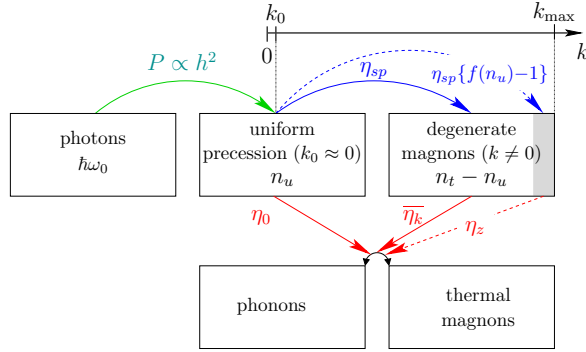


FIG. 2: Schematic diagram of the energy transfer between the various spin-waves modes. Alterations by non-linear effects (shaded area and dashed lines) are explicitly shown. Transfers between the upper reservoirs conserve the total energy. The coherent motion follows the equation of motion  $\dot{n}_u = \kappa P_{\text{abs}} - (\eta_0 + \eta_{sp})n_u - \eta_{sp}\{f(n_u) - 1\}n_u$ . Translated into Bloch's equation, the linear part of the schematic corresponds [14] to  $1/T_2 = (\eta_0 + \eta_{sp})/2$  and  $1/T_1 = (\eta_0 + \eta_{sp})/(1 + \eta_{sp}/\overline{\eta_k})$ , respectively the transverse and longitudinal relaxation rates.

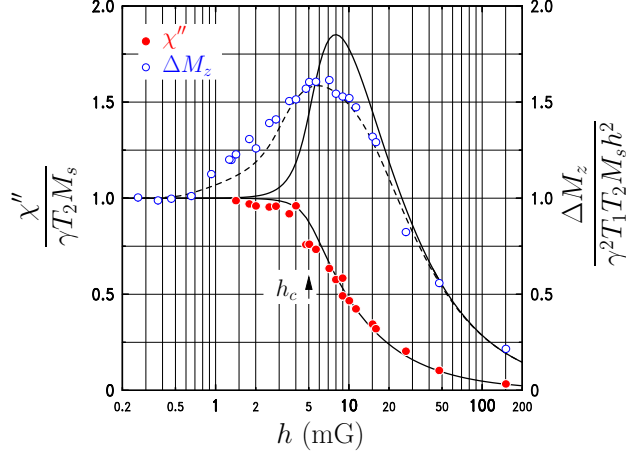


FIG. 3: Microwave field strength dependence of the transverse and longitudinal components of the magnetization at 10.47GHz. The solid lines are the behaviors predicted by the Suhl model when  $\eta_z = 0.15G$ . The dashed line is the same prediction convoluted by the spatial distribution of  $\Delta M_z$ . The quantities  $T_1$  and  $T_2$  are defined in the caption of Fig.2.

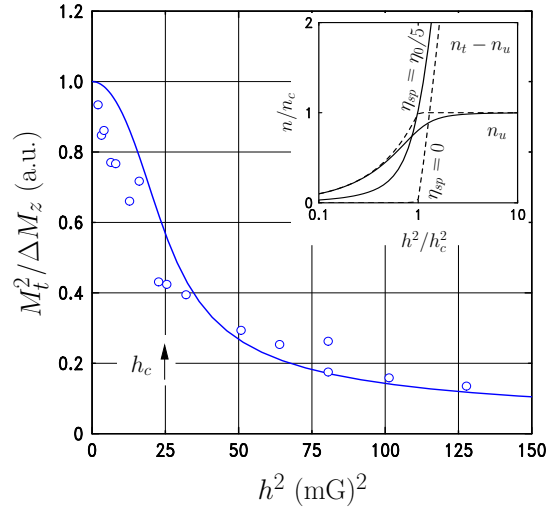


FIG. 4: Power dependence of the ratio of  $M_t^2 = \chi''^2 h^2$  over  $\Delta M_z$ . This ratio measures  $\tilde{\eta}_z$  the decay rate of the non-linear magnons pairs. The solid line is the predicted behavior within a first order approximation. Insert: Predicted power dependence of  $n_u$  and  $n_t$  for  $\eta_{sp}$  equals to  $\eta_0/5$  and 0.